University of Groningen

The AGN contribution to the UV-FIR luminosities of interacting galaxies and its role in identifying the Main Sequence

Ramos P, Andrés F.; Ashby, M. L. N.; Smith, Howard A.; Martínez-Galarza, Juan R.; Beverage, Aliza G.; Dietrich, Jeremy; Higuera-G, Mario-A; Weiner, Aaron S.

IMPORTANT NOTE: You are advised to consult the publisher's version (publisher's PDF) if you wish to cite from it. Please check the document version below.

Document Version
Publisher's PDF, also known as Version of record

Publication date:
2020

[Link to publication in University of Groningen/UMCG research database](#)

ELSEVIER

A 2D [Fe^{II}-bistetrazole] coordination polymer exhibiting spin-crossover properties

Manuel Quesada [a], Ferry Prins [a], Olivier Roubeau [b], Patrick Gamez [a], Simon J. Teat [c], Petra J. van Koningsbruggen [d], Jaap G. Haasnoot [a,*], Jan Reedijk [a,*]

[a] Leiden Institute of Chemistry, Gorlaeus Laboratories, Leiden University, P.O. Box 9502, 2300 RA Leiden, The Netherlands
[b] Centre de Recherche Paul Pascal-CNRS UPR 8641, 115 avenue du dr. A. Schweitzer, 33600 Pessac, France
[c] ALS, Berkeley Laboratory, 1 Cyclotron Road, MS2-400, Berkeley, CA 94720, USA
[d] University of Groningen, Stratingh Institute of Chemistry and Chemical Engineering, Nijenborgh 4, NL-9747 AG Groningen, The Netherlands

Abstract

The reaction of 1,3-bis(tetrazol-1-yl)-2-propanol (btzpol) with Fe(BF$_4$)$_2 \cdot$ 6H$_2$O in acetonitrile yields the remarkable 2D coordination polymer [Fe^{II}(btzpol)$_{1.8}$(btzpol-OBF$_3$)$_{1.2}$](BF$_4$)$_{0.8} \cdot$ (H$_2$O)$_{0.8}$(CH$_3$CN) (**1**). This compound has been structurally characterized using an X-ray single-crystal synchrotron radiation source. The iron(II) centers are bridged by means of double btzpol bridges along the c direction, and by single btzpol bridges along the b direction. The reaction of part of the ligand with the counterion has forced the compound to crystallize in this extended two dimensional structure. The compound shows spin-transition properties, both induced by temperature and light, with $T_{1/2} = 112$ K and $T(LIESST) = 46$ K, respectively. The relaxation of the metastable high-spin state created by irradiation is exponential, following an Arrhenius type behavior at high temperature, and dominated by a temperature independent tunneling process at lower temperatures.
© 2006 Elsevier B.V. All rights reserved.

Keywords: Iron(II); Spin-transition; Azole ligands; Metal-organic framework; LIESST; Relaxation

1. Introduction

The search for materials with predefined and tuneable properties has for long been appealing for scientists. In the 1970s, Schmidt has observed that the physical properties of a crystalline solid are both dependent on the properties of the individual molecular components and on the distribution of these molecules in the crystal lattice [1]. This search for a control over the "overall structure" has then been further explored by Wells with the "node and spacer" approach, defining the inorganic networks in terms of their topology [2], and was brought to the field of coordination polymers by Robson [3–5]. The porosity of these coordination polymers was exploited initially to develop the field of inclusion chemistry, motivated by applications in storage and catalysis [6]. Different types of linkers and coordination geometries at the metal centers are used to rationally obtain predetermined structural properties such as the size and shape of the cavities [7]. New challenges within this field involve the design of reticular networks, which now exhibit a functional property [8]. These hybrid inorganic–organic materials have already opened routes towards the obtaining of, for instance, active catalysts, enantiomeric separation, bistable systems, or for solid state synthesis [9–16].

The incorporation of the spin-crossover (SCO) property in reticular networks has also been investigated [11,17].

Light, temperature or pressure can be used as external stimuli to induce the entropy driven transition from the low-spin state (LS, $S = 0$) to the high-spin state (HS, $S = 2$) [18,19]. A change in size of the metal center is associated with the difference in electronic distribution. The distortions arising from this structural change may then be elastically propagated through the lattice [18,20]. The properties of the transition depend drastically on the efficiency of this cooperative behavior and thus, its control is paramount to designing these materials.

The majority of the spin-crossover compounds known until now are mononuclear species, and only a few polymeric species have been reported. 4-Substituted 1,2,4-triazole-based materials have extensively been used to covalently bind the Fe^{II} centers to produce 1D coordination polymers displaying cooperative SCO behavior [21–31]. 1,2,4-Triazole ligands have also yielded 2D ([Fe(btr)$_2$(NCX)$_2$], btr = 4,4′-bis-1,2,4-triazole; X = S [32,33], or Se [34], and 3D ([Fe(btr)$_3$](ClO$_4$)$_2$, btr = 4,4′-bis-1,2,4-triazole) systems [35], with a spin-crossover. Fe(II) spin-crossover materials having rigid 1D, 2D or 3D structures have been synthesized with cyanometallate organometallic linkers [36–39]. Other well-known ligands in this field are the tetrazoles [18]. Their bridging analogues, the bistetrazoles, are well established ligands to generate polymeric species with a wide variety of geometries and conformations [40,41]. It seems that the dimensionality of the resulting compound is imposed by the length, conformation and flexibility of the spacer linking the terazole moieties [42]. 1,2-Bis(tetrazol-1-yl)alkanes ($n = 1$–3) have yielded 1D polymers with gradual spin-transitions due to the shock absorber property of the alkane and their column style packing [40,43]. The increase of the spacer length to 4 carbons has yielded 3D catenane structures [42,44].

Although LIESST had been observed previously for iron (III) compounds in solution [45,46], the interesting optical properties of solid-state iron spin-crossover compounds were discovered in 1984 [47]. Decurtins et al. reported the LIESST effect (light induced spin state trapping) and since then, many studies have been dedicated to the understanding of its mechanism [18,48]. Among polymeric species, [Fe(btzp)$_3$](ClO$_4$)$_2$ (btzp, 1,2-bis(tetrazol-1-yl)propane) was the first one dimensional polymer to show the LIESST effect [40]. In addition, [Fe(btzb)$_3$](ClO$_4$)$_2$ (btzb,1,4-bis(tetrazol-1-yl)butane) [42], as well as polymeric materials with cyanide building blocks have been found to display LIESST [36,39]. The stability of the high-spin metastable state has not yet been studied for bistetrazole derivatives.

Herein, we report on the synthesis, structure and physical properties of a 2D iron(II) spin-crossover complex based on a new bistetrazole ligand (btzpol, 1,3-bis(tetrazol-1-yl)-2-propanol). The coordination compound [Fe^{II}(btzpol)$_{1.8}$(btzpol-OBF$_3$)$_{1.2}$](BF$_4$)$_{0.8}$ · (H$_2$O)$_{0.8}$(CH$_3$CN) (1) is obtained from irom(II) tetrafluoroborate and the ligand, and exhibits a partial reaction of tetrafluoroborate with a non-coordinating part of the ligand (Fig. 1). Studies on the LIESST and relaxation kinetics of the metastable HS state of this compound are also presented.

2. Experimental

2.1. General

All reagents were used as received. Elemental analyses (C, H, N) were carried out on a Perkin–Elmer 2400 series II analyzer. Magnetic susceptibility measurements (6–300 K) were carried out using a Quantum Design MPMS-5S SQUID magnetometer, in a 1 kG applied field. Data were corrected for the experimentally determined contribution of the sample holder. Corrections for the diamagnetic responses of the complex, as estimated from Pascal's constants, were applied [49]. LIESST experiments were performed within the SQUID cavity by use of a 110 W halogen lamp and a green–blue filter (300–600 nm). Light was driven through a Y-shaped optical fiber that replaced the usual insert. The ligand field spectrum of the solid compound was recorded in the 300–1200 nm range on a Perkin–Elmer λ 900 spectrophotometer using the diffuse reflectance technique, with MgO as a reference.

2.2. Crystallographic studies

Measurements were made using Si(111) monochromated synchrotron radiation ($\lambda = 0.6894$ Å) and a Bruker APEX II CCD diffractometer using standard procedures and programs for Station 9.8 of Daresbury SRS [50]. Data were collected on a Bruker APEX II CCD diffractometer using the APEX 2 software and processed using SAINT v7.06a [51]. The crystal was mounted onto the diffractometer at low temperature under nitrogen at ca. 150 K. The structure was solved using direct methods with the SHELXTL program package. All non-hydrogens were refined anisotropically except partial water oxygen atoms and O1 and O1′. Displacement parameter restraints were used in modeling the BF$_4$. Geometrical restraints were used in modeling the OH and OBF$_3$ disorder. Hydrogens were
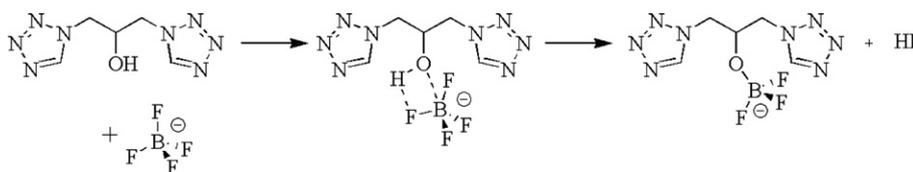

Fig. 1. Schematic illustration of the reaction between *btzpol* and the tetrafluoroborate anion.

placed geometrically where possible. It proved impossible to place or find the OH, water and acetonitrile hydrogens and so they were omitted from the refinement ($U_{ij} = 1.2$ U_{eq} for the atom to which they are bonded (1.5 for methyl)). The function minimized was $[w(F_o^2 - F_c^2)]$ with reflection weights $w - 1 = [2F_o^2 + (g_1 P) + (g_2 P)]$ where $P = [\max F_o^2 + F_c^2]/3$.

2.3. Synthesis of 1,3-bis(tetrazol-1-yl)-2-propanol (btzpol)

25 g (0.278 mol) of 1,3-diamino-2-propanol, 354 g (2.38 mol) of triethylorthoformate, and 41.5 g (0.639 mol) of sodium azide were dissolved in 400 ml of acetic acid and heated at 90 °C for 2 days. After cooling, HCl (conc.) was added to the solution and a first crop of compound, i.e. the monotetrazole (1-amino-3-(1H-tetrazol-1-yl)propan-2-ol) derivative was isolated by filtration and discarded. The filtrate was then dried and columned (Eluent: MeOH 10/CH$_2$Cl$_2$ 90). The pure product was obtained in 10% yield (m = 5.45 g). ^{1}H NMR (300 MHz, DMSO-d_6) δ: 4.30 (m, 1H, tz-CH$_2$–CH), 4.43 (dd, 2H, tz-CH$_2$), 4,70 (d, 2H, tz-CH$_2$), 9,32 (s, 2H, tz-H5). *Anal.* Calc. for C$_5$H$_8$N$_8$O: C, 30.61; N, 57.12; H, 4.11. Found: C, 29.79; N, 57.15; H, 4.37%.

2.4. Preparation of [Fe^{II}(btzpol)$_{1.8}$(btzpol-OBF$_3$)$_{1.2}$]-(BF$_4$)$_{0.8}$ · (H$_2$O)$_{0.8}$(CH$_3$CN) (1)

50 mg (0.26 mmol) of btzpol dissolved in 5 ml of acetonitrile were added to 29 mg (0.085 mmol) of Fe(BF$_4$)$_2$ · 6H$_2$O dissolved in 5 ml of acetonitrile. The solution was heated for an hour at 50 °C, after which the solution was allowed to stand at room temperature. Colorless single crystals appeared after 2 days under slow evaporation of the solvent, at room temperature. The white crystals were then washed with acetonitrile. Yield: 10%. *Anal.* Calc. for [(1)-(H$_2$O)–0.5 · (CH$_3$CN)] C$_{17}$H$_{28.2}$B$_2$F$_{6.8}$FeN$_{25}$O$_{4.2}$: C, 23.59; N, 42.13; H, 3.01. Found: C, 23.25; N, 42.35; H, 2.96%.

3. Results and discussion

3.1. X-ray Structure of [Fe^{II}(btzpol)$_{1.8}$(btzpol-OBF$_3$)$_{1.2}$]-(BF$_4$)$_{0.8}$ · (H$_2$O)$_{0.8}$(CH$_3$CN)

[Fe^{II}(btzpol)$_{1.8}$(btzpol-OBF$_3$)$_{1.2}$](BF$_4$)$_{0.8}$ · (H$_2$O)(CH$_3$CN) crystallizes in the space group $P2_1/m$, with $Z = 2$. The asymmetric unit consists of an Fe^{II} ion on a special position, a btzpol ligand, a slightly modified ligand btzpol-OBF$_3$ in which the alcohol moiety has reacted with a tetrafluoroborate anion, and a ligand that presents an occupational disorder between OH/OBF$_3$ in a 1:5 ratio. Table 1 includes the most relevant crystallographic parameters. A view of the iron(II) coordination sphere and atom labeling is depicted in Fig. 2.

The metal center is hexacoordinated by six N tetrazole donors belonging to six different ligands. Two of these six bistetrazole ligands are covalently bond to a BF$_3$ moiety

Table 1
Crystallographic data for [Fe(btzpol)$_{1.8}$(btzpol-OBF$_3$)$_{1.2}$](BF$_4$)$_{0.8}$ (1)

Empirical formula	C$_{17}$H$_{28.20}$B$_2$F$_{6.80}$FeN$_{25}$O$_{4.20}$
Formula weight	856.72
Temperature (K)	150
λ (Å)	0.6894
Space group	$P2_1/m$
Z	2
a (Å)	7.1402(4)
b (Å)	24.0050(15)
c (Å)	10.6885(7)
V (Å^3)	1831.77(19)
ρ (g/cm^3) calculated	1.553
$R(F)^a$	0.0719
$R_w(F^2)^a$	0.2132

^{a} $R_1 = \Sigma ||F_o| - |F_c||/\Sigma |F_o|$

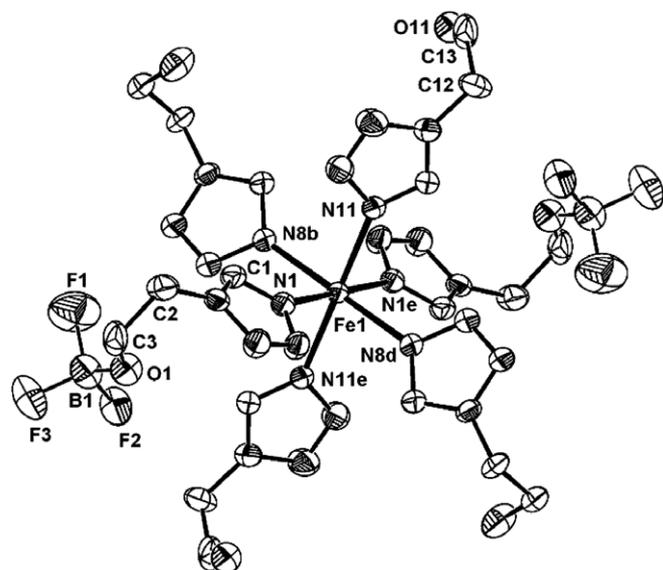
Fig. 2. Labeled ORTEP representation of the iron coordination sphere of [Fe^{II}(btzpol)$_{1.8}$(btzpol-OBF$_3$)$_{1.2}$](BF$_4$)$_{0.8}$ · (H$_2$O)(CH$_3$CN) (1). Hydrogen atoms, solvent molecules and counterions are not shown for clarity. Letters are used to indicate symmetry related atoms; b = x, y, $1 + z$; d = $-x$, $1 - y$, $1 - z$; e = $-x$, $1 - y$, $2 - z$.

through the alcoholic function. An almost perfect O_h symmetry is found around the iron(II) atom, with N–Fe–N angles ranging from 88.88(12)° to 91.12(12)° (see Table 2). The slight distortion observed is not unusual for Fe^{II} tetrazole compounds in the high-spin state. The Fe–N distances (2.169(3)–2.182(3) Å) are in the expected range for Fe^{II} in

Table 2
Hydrogen bond interactions for 1

Atoms	Distance (Å)
C(1)–H(1)···F(6)	2.27
C(2)–H(2B)···F(4)	2.52
C(4)–H(4A)···F(3)	2.52
Intra 1 C(5)–H(5)···F(3)	2.33
Intra 1 C(11)–H(11)···F(2)	2.34

the HS state. Along the *b* axis, the Fe–N distances are of 2.169 Å and 2.175 Å, slightly shorter than those along the *c* axis, but still in the range of Fe–N distances for a high-spin iron(II) compound.

This iron coordination entity consists of a building unit to form a two-dimensional network in which the Fe^{II} ions are connected through single 1,3-bis(tetrazol-1-yl)-2-propanol (btzpol) bridges in the *b* direction, and by means of double ligand bridges in the *c* direction (Fig. 3). Along the latter direction, one of the two ligands is a btzpol-OBF_3, formed from reaction between the ligand and the tetrafluoroborate.

The other ligand presents an occupational disorder [40,52], in which the OBF_3/OH occupancy ratio is 1:5. This peculiar feature explains the fractional numbers present in the molecular formula. The representation shown in all figures is therefore the major component of the disordered structure. The BF_4^- anions are interacting by means of hydrogen-bond forces with the hydrogen atoms of the ligands along the *c* direction (Table 2).

The bridging ligand in the c direction (Fig. S1) has a gauche-gauche (GG) conformation when viewed along C12···C13 and C13···C14 axes, respectively, with an N11···N11g separation of 8.433(4) Å. The Fe1–N11 bond distance is 2.182(3) Å (see Table 3). Since the btzpol ligands are bridging the iron centers (Fe1···Fe1c; 12.0025(8) Å) in a zigzag fashion, the alcohol functions are alternatively pointing in opposite directions. These alcohol moieties do not show any type of intermolecular contact with other molecules present in the lattice.

The view along the *b* axis shows another remarkable feature of the coordination polymer (Fig. 4). The two btzpol

Table 3
Selected bond lengths (Å) and angles (°) for **1**

Fe–Fe (double ligand bridge)	10.6885(7)
Fe–Fe (single ligand bridge)	12.0025(8)
N1–N8	7.647(5)
N11–N11g	8.433(4)
Fe1–N1	2.175(3)
Fe1–N11	2.182(3)
Fe1–N8d	2.169(3)
N1–Fe1–N1e	179.997
N1–Fe1–N8b	89.61
N1–Fe1–N8d	90.39
N1–Fe1–N11	90.78
N1–Fe1–N11e	89.22
N8d–Fe1–N8b	180.0
N8d–Fe1–N11	91.12
N8d–Fe1–N11e	88.88
N11e–Fe1–N11	180.00

Letters are indicating symmetry related atoms; b = x, y, 1 + z, d = −x, 1 − y, 1 − z, e = −x, 1 − y, 2 − z and g = x, 3/2 − y, z.

ligands bridging the iron centers (Fe1···Fe1a; 10.6885(7) Å) along the *c* axis have a *trans*-gauche (TG′) conformation [53], if viewed along the C12···C13 and C13···C14 bonds, respectively, with a N1···N8 distance of 7.647(5) Å. The fact that two ligands bridge the iron centers results in a significant decrease of the distance of about 1.3 Å between the metal ions, as compared to the Fe–Fe separation observed along the *c* axis. However, the conformation of the ligand may also play a role in determining these distances, which will be discussed below. The alcohol function of one of the two bridging ligands has reacted with a BF_4^- anion. The resulting O–BF_3 group interacts with one of the tetrazole rings of the same ligand through anion–π
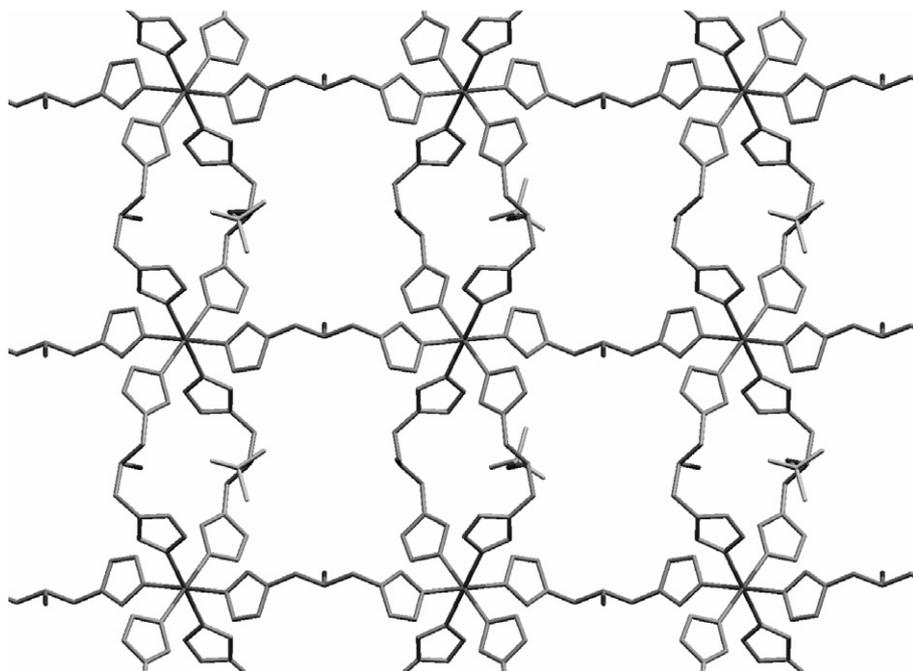

Fig. 3. Representation of the major component of the disordered 2D structure of **1** along the *a* axis. Hydrogen atoms, solvent molecules and counterions are not shown for clarity.
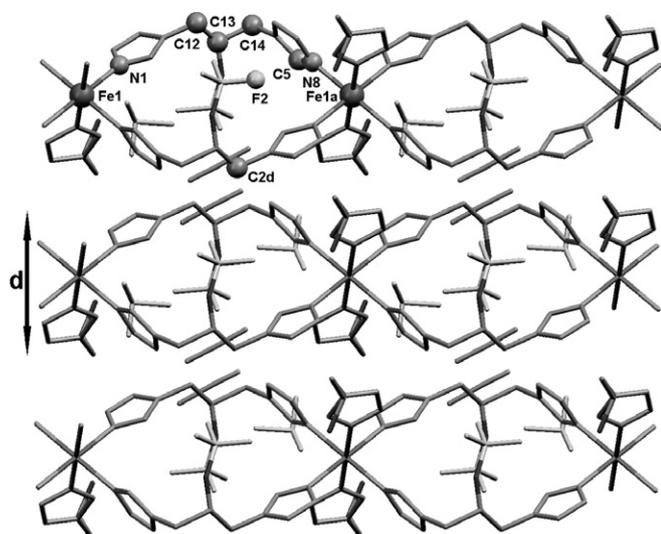
Fig. 4. Representation of **1** along the *b* axis. Hydrogen atoms are not shown. d is defined as (d, C14···C2d), see text. Letters are used to indicate symmetry related atoms; a = x, y, −1 + z and d = −x, 1 − y, 1 − z.

interactions (C5···F2 3.067(8) Å). A partial water molecule sitting in the cavity is dislocated in four positions (occupancy factor of 0.2 for each position). The 2D layers have a thickness (d, C4···C2d) of about 7.409(7) Å, produced by the two bridging ligands in this direction. No interactions between layers are observed, as neither solvent molecules nor counterions are sitting between the layers.

3.2. Magnetic studies

Magnetic data for a polycrystalline sample of **1** have been recorded in the temperature range 6–300 K. The $\chi_m T$ versus T plot is depicted in Fig. 5 (white circles) where χ_m is the molar magnetic susceptibility per iron center and T the temperature. At 300 K, the $\chi_m T$ value is 3.4 cm^3 mol^{-1} K, which is close to that expected for a spin-only HS iron center (3 cm^3 mol^{-1} K, g = 2). On cooling, the $\chi_m T$ value remains constant until a temperature of 200 K, where a gradual transition sets in, expanding over a temperature range of 130 K, after which it reaches a $\chi_m T$ value of 0.9 cm^3 mol^{-1} K at 50 K. At very low temperatures, a slight decrease in the $\chi_m T$ value is observed, which can only be assigned to the zero-field splitting of the remaining high spin iron centers. The temperature at which the molar fractions of the high-spin and low-spin molecules are equal to 0.5, $T_{1/2}$ is 112 K. This value represents a rather low transition temperature, although not unusual, since low $T_{1/2}$ have been observed for bistetrazole-based iron complexes [40], and especially for mononuclear tetrazole-based compounds [18,54–57].

3.3. LIESST and relaxation experiments

UV–Vis spectroscopic measurements at liquid nitrogen temperature (Fig. 6) indicate that the $^1A_1 \rightarrow {}^1T_1$ absorption
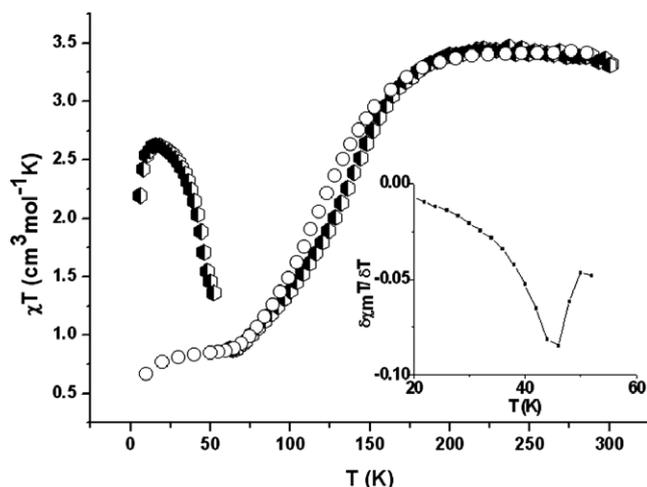

Fig. 5. Plot of experimental $\chi_m T$ vs. T for **1** (white circles). Temperature dependence of the product $\chi_m T$ after LIESST, in the 6–300 K range (black and white hexagons). The inset shows the derivative of the product $\chi_m T$.

band for LS Fe^{II} is situated at 555 nm; therefore a cut-off filter with transmittance below 559 nm has been used. Excitation with a green light at 6 K within the squid cavity creates the so-called high-spin metastable state, which is followed by the increase in magnetic response (Fig. 5). Times of excitation point at a low efficiency of the light-induced process, as more than 3 h of continuous irradiation are needed to reach saturation (namely a maximal population of the metastable HS state). The estimation of the exact percentage of metastable HS state formed is hampered by the fact that the $\chi_m T$ value at this temperature shows a large contribution from the zero-field splitting of HS Fe^{II} species. Consequently, the increase in $\chi_m T$ value on irradiation yields a $\chi_m T$ signal which holds the contributions from the newly created metastable HS form, as well as of its zero-field splitting. A $\chi_m T$ value of 2.2 cm^3 mol^{-1} K is obtained at 6 K, indicating by comparison with the high temperature $\chi_m T$
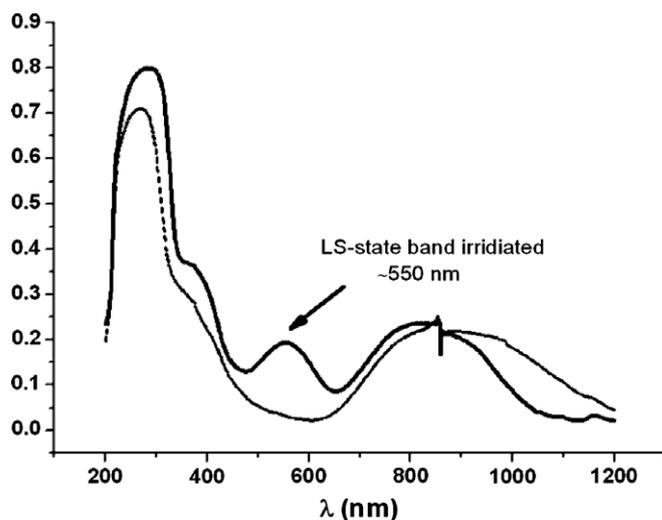

Fig. 6. UV–Vis spectra for **1** at room temperature (dashed lined), and at liquid N$_2$ temperature (full line).

data that a close to complete population of the metastable state is achieved. The skinning effect, due to the amount of sample used, and the inherent technical problems of irradiation experiments can account for the incompleteness of the population.

After having yielded the maximal population of the metastable HS state, i.e. a $\chi_m T$ value of 2.2 cm^3 mol^{-1} K, the temperature has been increased at a rate of 0.3 K/min with the lamp switched off. The initial increase of $\chi_m T$ reaching a value of 2.6 cm^3 mol^{-1} K seems to confirm that the low $\chi_m T$ value obtained during excitation is partly due to the presence, at this temperature, of a zero-field splitting effect. This phenomenon is observed until it is masked at 20 K by the relaxation of the metastable state, placing the $T(LIESST)$ value at 46 K (inset Fig. 5) [58]. A similar behavior is observed for the [Fe(nditz)$_3$](ClO$_4$)$_2$ bearing short alkyl spacers [59]. Relaxation kinetics of HS to LS conversion for the compound [Fe^{II}(btzpol)$_{1.8}$(btzpol-OBF$_3$)$_{1.2}$](BF$_4$)$_{0.8}$ · (H$_2$O)$_{0.8}$(CH$_3$CN) has been studied at different temperatures: 6, 12, 24, 36, 42 and 50 K. In all cases, the compound is excited at 6 K and then rapidly set to the corresponding next temperature. The $\chi_m T$ value is normalized [60] to $\gamma_{HS} = 1$. In the case of the highest temperature, part of the iron centers may have relaxed before the measurement has started, although this should not alter the value for the high-spin to low-spin relaxation rates (K_{HL}). The $\chi_m T$ value reflecting the decay in the percentage of metastable HS form is then measured every 30 s. Similarly shaped relaxation curves are obtained for 12, 24, 36 and 42 K, temperatures at which a total relaxation is not reached, even after several hours (Fig. 7). In contrast, at 50 K, the compound relaxes in a few hours. This result indicates that the compound is already in the thermally activated region. In this region, the compound may indeed populate higher vibrational states from which a more effective relaxation to the LS state occurs.
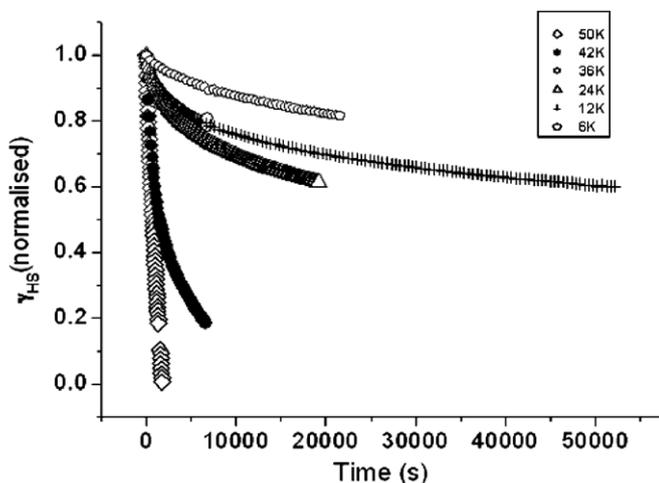

Fig. 7. HS → LS relaxation curves after LIESST at six different temperatures. Normalized as: $\chi_m T(t) - \chi_m T$ (LT)/$\chi_m T$ (Initial) − $\chi_m T$(LT). $\chi_m T$ (LT) = low temperature value obtained from the normal spin crossover curve; $\chi_m T$ (Initial) = value after population of the metastable high-spin state.

3.4. Discussion

[Fe^{II}(btzpol)$_{1.8}$(btzpol-OBF$_3$)$_{1.2}$](BF$_4$)$_{0.8}$ · (H$_2$O)$_{0.8}$(CH$_3$CN) is a 2D SCO polymer based on bistetrazole-type ligands. Bistetrazoles are widely used in reticular synthesis combined with different metals. Copper, nickel and zinc complexes have shown different topologies, and 1D, 2D, or 3D structures have been reported [61–63]. The use of Fe^{II} as the metal ion not only generates unique supramolecular networks, but may also produce spin-transition compounds. 1-Substituted tetrazoles provide the proper crystal field splitting to form spin-transition materials. In this respect, all bistetrazole-based spin-transition compounds previously reported do present 1D or 3D networks [41]. The present coordination polymer is thus the first 2D bistetrazole-based material exhibiting such magnetic properties.

The synthesis of complexes with tetrafluoroborate counterions may yield products where the instability of the anion is observed [64,65]. Stable hydrogen–bonding interactions between the fluoride atoms and protons of donor ligands [66] can indeed result in the formation of HF molecules. The ensuing fluorine atoms may then act as ligands and form unexpected complexes [67]. In the present case, the btzpol ligand, through its alcohol functions, provides the H atoms, creating an R–O–H · (F$_n$)BF$_{4-n}$ nucleophile (Fig. 1) [66]. The elimination of HF molecules gives rise to the formation of a stable R–O–BF$_3$ entity. This phenomenon which has already been reported [66,68], generates a slightly modified ligand which bridges the iron centers through the N1 of the tetrazole rings. In this instance, it has been proven through repetitive synthesis of the material, that the composition and physical behavior (see below) are reproducible, indicating that the formation of the OBF$_3$ ligand always takes place under these experimental conditions.

In bis(4-pyridyl)alkanes, the length of the spacer and its conformation seem to play an important role in determining the dimensionality of the compound [69]. In bis(polyazole) derivatives, such as bistetrazoles, an additional factor is present, namely the free rotation of the azole ring around the ring-spacer bond [53]. This free rotation influences the N4···N4′ distance (coordinated nitrogens of the bis(tetrazole) ligand), and thus will also affect the important structural features of the resulting coordination architectures, such as dimensionality, interpenetration, and size of the cavity. Ultimately, this free rotation will influence as well the properties of the SCO.

Recently, copper(II) and zinc(II) coordination polymers prepared with the 1,3-bis(tetrazol-2-yl)propane ligand were reported [53]. These studies demonstrate that the metal–metal distance in alkylbis(polyazole)-based polymers only depends on the spacer length and not on its conformation. In fact, the difference in distances owing to the distinct conformations is compensated by the tilting of the N(ring)–C(spacer) bond, resulting in an N4···N4′ distance difference of 0.188 Å between the two disparate conformers

(which is considered as negligible). In the present study, two types of conformation are observed for the ligands, i.e. a TG′ conformation along the *b* axis (double ligand bridge) and a GG conformation along the *c* axis (single ligand bridge). The disparity between the N4···N4′ and M···M distances of the two ligands is 0.786 Å and 1.314 Å, respectively. The reaction of the ligand with the tetrafluoroborate anion to form the altered ligand btzpol-OBF_3 appears to be responsible for these significant differences in distances between the two ligands. The presence of the more bulky OBF_3 moiety stabilizes the coordination network through anion–π interactions (C5···F2 3.067(8) Å) between the fluoride atoms and the electro-deficient tetrazole rings. Moreover, these anion–π interactions annihilate the rotational freedom of the tetrazole around the N(ring)–C(spacer) bond, which is believed to be responsible for the compensation of the difference in N4···N4′ distance between different conformers [53]. These features are most likely the origin of the important difference in the N4···N4′ distances observed in the solid-state structure. The presence of the linked OBF_3 moieties is apparently responsible for the formation of the 2D framework obtained. Bistetrazole ligands bearing a short linear alkyl spacer (2 carbon spacer) with a *syn* conformation lead to the formation of 1D coordination polymers [43], like [$Fe(endi)_3$](BF_4)$_2$ (endi = 1,2-bis(tetrazol-1-yl)ethane) or [$Cu(btze)_3$](ClO_4)$_2$ (btze = 1,2-bis(tetrazol-1-yl)ethane). In the present complex, a third btzpol-OBF_3 ligand or a btzpol ligand cannot obviously bind to the metal ion along the same direction, due to the steric constraints brought in by the R–OBF_3 group. As a result, the binding of the third ligand, i.e. btzpol, can only extend the coordination structure along another direction, resulting in this peculiar 2D layered architecture.

Tetrazole-based ligands are known to center the spin-transition at relatively low temperatures. The current transition at 112 K, accompanied by a pronounced thermochromic effect, is therefore not surprising. In a recent systematic study on a series of Fe^{II} compounds based on bistetrazole ligands with alkyl chains as spacers, a linear relation between the number of carbons and the $T_{1/2}$ has been found; moreover, a dependence on the parity of the chain has also been observed [59]. Although this compound is not a 3D structured compound, the $T_{1/2}$ value follows this trend. This seems reasonable as the dimension of the polymer formed has not been found to affect the $T_{1/2}$ of the transition, and appears only to depend on the nature of the ligand itself [59]. Nevertheless, this case represents one of the lowest transition temperatures reported until now [54,55]. In the present study, the relatively high percentage of iron centers that do not undergo the transition is reproducible over different samples and is independent of the cooling rate. It is hence not related to impurities nor trapping in HS state. Structural defects within the solid-state framework therefore constitute a possible explanation of the incompleteness of the transition. Another reasonable possibility is that the structural

changes associated with the spin transition, e.g. the contraction of the crystal lattice, restricts the number of Fe^{II} ions capable of switching from HS to LS. This can explain that the remnant HS value at low temperatures is always similar. Both explanations can account for this effect.

The cooperativity in spin-crossover materials is a desired property as it leads to steeper transitions and, in some cases, to hysteresis effects. This cooperative behavior results from the structural changes associated with the transition, which are elastically communicated throughout the lattice. The gradual transition observed for [Fe^{II}(btzpol)$_{1.8}$(btzpol-OBF_3)$_{1.2}$](BF_4)$_{0.8}$ · (H_2O)$_{0.8}$(CH$_3$CN), indicates that the flexibility of the 2D network is hampering the propagation of the structural changes intrinsic to the transition [70,71]. Normally, it is through rigid linkers [72], or via an efficient crystal packing [42,44] that the rigidity is achieved in coordination polymers. In the present investigation, the btzpol ligand has an alkyl-based spacer which confers flexibility to the ligand, and thus acts as a shock absorber, as in the case of [$Fe(endi)_3$](BF_4)$_2$ [40]. At the same time, [Fe^{II}(btzpol)$_{1.8}$(btzpol-OBF_3)$_{1.2}$](BF_4)$_{0.8}$ · (H_2O)$_{0.8}$(CH_3CN) does not form a catenane structure and its BF_4^- anions, sitting in the cavities, do not completely occupy the space. This allows the ligand to perfectly adapt its conformation in order to counterbalance the molecular distortions created by the SCO. Unfortunately, the use of other counterions that would maybe fill up the voids, namely Cl^-, ClO_4^-, and PF_6^-, has not yielded spin-transition materials. Furthermore, no intermolecular interactions between the 2D sheets are observed, resulting in less rigid structures.

The features of the transition indicate that the metastable high-spin state can be observed at low temperatures. The low transition temperature and the lack of cooperativity enhance the stability of this metastable state. Indeed, this is observed when the compound is excited with a green light during long excitation times. These long excitation times required can be explained by a skinning effect and/or a low intensity light emission. The slight incompleteness of the population of the metastable HS state, and the presence of zero-field splitting for HS Fe^{II} species (upon excitation at 6 K), leads to a $\chi_m T$ value, which is lower than the expected one for an Fe^{II} center. Once the light is turned off and the temperature is slowly increased (see Fig. 5), the relaxation sets in gradually. This indicates that part of the iron centers relax earlier and faster than the bulk majority. Consequently, a thermally activated process cannot account for this initial decay of the metastable HS form. Actually, this effect can be attributed to the lack of homogeneity, most likely as a result of the occupational disorder of the OH/OBF_3 moiety in one of the ligands. This gives rise to slightly different Fe^{II} SCO chromophores with slightly disparate transition temperatures and hence different relaxation rates [15]. This matches with the fact that before the measurement has started, the relaxation rates show a fast

decay to the low spin state of a small fraction of the iron centers (normalized to 1) [60].

A relatively high $T(LIESST)$ [58] of 46 K is found experimentally with a heating rate of 0.3 K/min for **1**. Based on Letard's study [73], for monodentated compounds, the $T(LIESST)$ and the $T_{1/2}$ relate as

$$T(LIESST) = T_0 - 0.3T_{1/2}. \tag{1}$$

For the present compound $[Fe^{II}(btzpol)_{1.8}(btzpol-OBF_3)_{1.2}]-(BF_4)_{0.8} \cdot (H_2O)_{0.8}(CH_3CN)$, it does follow the expected trend as it lies close to the $T_0 = 100$ K line (monodentated ligands). A value of 66 K is obtained for $T(LIESST)$ when using (Eq. (1)); the difference with the experimental value can be due to the fact that this compilation does not consider any polynuclear material. The study of the relaxation rates of bistetrazole-based compounds has not been performed yet. Single exponential relaxation curves are found for all the temperatures studied (Fig. 7). The relaxation data were fitted to an exponential decay equation to obtain the relaxation constant values (K_{HL}) (Table 4), which were then charted as an Arrhenius plot (Fig. S2).

The curve obtained exhibits two distinct parts, corresponding to the two different relaxation regions. At high temperatures, the relaxation constant is dependent on the temperature and follows a simple Arrhenius behavior. This is the so-called thermally activated region where the relaxation can be considered as occurring from excited vibrational states. At low temperatures, a deviation from the simple Arrhenius behavior is observed, as the relaxation constant does not practically depend on the temperature. This behavior is characteristic of a low-temperature tunneling process. The curvature is due to the overlap of both regions.

Considering the high-temperature region (from 36 to 50 K), an Arrhenius fit (Fig. S2) results in a very low activation energy value (E_a). As the energy difference between the two lowest vibrational levels of the HS state and the LS state is directly dependent on the $T_{1/2}$ [48,74], such a low transition temperature (112 K) indicates that both states are close in energy. Thus, one would expect a higher activation energy for this compound. The slight deviation from linearity observed in the temperature range 36–50 K evidences the presence of tunneling, which is probably behind the low E_a value obtained [74]. Indeed, the low value obtained for the pre-exponential factor A confirms a dominant tunneling effect [37]. Relaxation curves recorded at

higher temperatures would be needed to obtain a more accurate value.

4. Concluding remarks

The reaction of bistetrazole-based ligands with Fe^{II} usually leads to the formation of 1D or 3D spin-transition polymers, depending on the length and/or the conformation of the spacer involved. The present ligand 1,3-bis(tetrazol-1-yl)-2-propanol btzpol, has demonstrated that a 2D spin-transition polymer can be obtained with bistetrazole-based ligands. Two btzpol ligands bind along the same axis forming a 1D polymer, as for the previously reported cases with short spacers (2-carbon links), but the unexpected reaction of the btzpol ligand with the tetrafluoroborate has forced the third bridging ligand to accommodate along a different axis, forming a 2D polymer. The distortion on the bistetrazole conformation created by the R–OBF_3 moiety, and its implicit bulkiness explain the singular disposition adopted by the compound. $[Fe^{II}(btzpol)_{1.8}(btzpol-OBF_3)_{1.2}](BF_4)_{0.8} \cdot (H_2O)(CH_3CN)$ shows spin-crossover properties induced with both temperature and light. This first study of the relaxation behavior of the metastable HS state carried out for this type of polymer proves that it follows a nearly temperature-independent rate at low temperatures (<36 K) and a thermally activated behavior at higher temperatures (>36 K). There is an obvious overlap between the two regions, which results in low kinetic values for the temperature activated behavior. The low degree of cooperativity in the SCO characteristics of the polymer can be explained by the space present in the form of cavities, which permits the flexible btzpol (btzpol-OBF_3) to absorb the structural changes associated with the spin transition. The use of alcohol moieties in the search of intermolecular interactions that would bring an extra rigidity to the material has been surprisingly disrupted by the peculiar reaction with the counterion. This R–OBF_3 moiety has been dominating the overall structure and thus the properties of the material.

Table 4
HS to LS relaxation rates after quantitative LIESST effect performed at 6 K

Temperature (K)	K_{HL} (10^{-4} s^{-1})
50	3.57
42	5.37
36	3.2
24	1.4
12	0.58
6	0.725

Appendix A. Supplementary material

CCDC 633410 contains the supplementary crystallographic data for **1**. These data can be obtained free of charge via http://www.ccdc.cam.ac.uk/conts/retrieving.html or from the Cambridge Crystallographic Data Centre, 12 Union Road, Cambridge CB2 1EZ, UK; fax: +44 1223-336-033; or e-mail: deposit@ccdc.cam.ac.uk. Supplementary data associated with this article can be found, in the online version, at doi:10.1016/j.ica.2006.12.010.

References

[1] G.M. Schmidt, Pure Appl. Chem. 27 (1971) 647.
[2] A.F. Wells, J. Chem. Educ. 54 (1977) 273.
[3] B.F. Abrahams, B.F. Hoskins, J.P. Liu, R. Robson, J. Am. Chem. Soc. 113 (1991) 3045.
[4] S.R. Batten, B.F. Hoskins, B. Moubaraki, K.S. Murray, R. Robson, J. Chem. Soc., Dalton Trans. 17 (1999) 2977.
[5] B.F. Hoskins, R. Robson, J. Am. Chem. Soc. 112 (1990) 1546.
[6] M. Fujita, Y.J. Kwon, S. Washizu, K. Ogura, J. Am. Chem. Soc. 116 (1994) 1151.
[7] O.M. Yaghi, M. O'Keeffe, M. Kanatzidis, J. Solid State Chem. 152 (2000) 1.
[8] N.L. Rosi, J. Eckert, M. Eddaoudi, D.T. Vodak, J. Kim, M. O'Keeffe, O.M. Yaghi, Science 300 (2003) 1127.
[9] H.K. Chae, D.Y. Siberio-Perez, J. Kim, Y. Go, M. Eddaoudi, A.J. Matzger, M. O'Keeffe, O.M. Yaghi, Nature 427 (2004) 523.
[10] M. Eddaoudi, J. Kim, N. Rosi, D. Vodak, J. Wachter, M. O'Keefe, O.M. Yaghi, Science 295 (2002) 469.
[11] G.J. Halder, C.J. Kepert, B. Moubaraki, K.S. Murray, J.D. Cashion, Science 298 (2002) 1762.
[12] S. van Zutphen, M.S. Robillard, G.A. van der Marel, H.S. Overkleeft, H. den Dulk, J. Brouwer, J. Reedijk, Chem. Commun. (2003) 634.
[13] O. Ohmori, M. Fujita, Chem. Commun. (2004) 1586.
[14] O. Ohmori, M. Kawano, M. Fujita, J. Am. Chem. Soc. 126 (2004) 16292.
[15] O. Kahn, C.J. Martinez, Science 279 (1998) 44.
[16] J.S. Seo, D. Whang, H. Lee, S.I. Jun, J. Oh, Y.J. Jeon, K. Kim, Nature 404 (2000) 982.
[17] J.-A. Real, E. Andrés, M.C. Muñoz, M. Julve, T. Granier, A. Bousseksou, F. Varret, Science 268 (1995) 265.
[18] P. Gütlich, A. Hauser, H. Spiering, Angew. Chem., Int. Ed. Engl. 33 (1994) 2024.
[19] M. Sorai, S. Seki, J. Phys. Chem. Solids 35 (1974) 555.
[20] H. Spiering, Top. Curr. Chem. 235 (2004) 171.
[21] C. Jay, F. Grolière, O. Kahn, J. Kröber, Mol. Cryst. Liq. Cryst. Sci. Technol. Sect. A – Mol. Cryst. Liq. Cryst. 234 (1993) 255.
[22] J.G. Haasnoot, Coord. Chem. Rev. 200 (2000) 131.
[23] Y. Garcia, P.J. van Koningsbruggen, R. Lapouyade, L. Fournès, L. Rabardel, O. Kahn, V. Ksenofontov, G. Levchenko, P. Gütlich, Chem. Mater. 10 (1998) 2426.
[24] E. Codjovi, L. Sommier, O. Kahn, C. Jay, New J. Chem. 20 (1996) 503.
[25] Y. Garcia, P.J. van Koningsbruggen, E. Codjovi, R. Lapouyade, O. Kahn, L. Rabardel, J. Mater. Chem. 7 (1997) 857.
[26] P.J. van Koningsbruggen, Y. Garcia, E. Codjovi, R. Lapouyade, O. Kahn, L. Fournès, L. Rabardel, J. Mater. Chem. 7 (1997) 2069.
[27] O. Kahn, E. Codjovi, Y. Garcia, P.J. van Koningsbruggen, R. Lapouyade, L. Sommier, Acs. Sym. Ser. 644 (1996) 298.
[28] O. Kahn, E. Codjovi, Philos. Trans. R. Soc. Lond. Ser. A – Math. Phys. Eng. Sci. 354 (1996) 359.
[29] L.G. Lavrenova, V.N. Ikorskii, V.A. Varnek, I.M. Oglezneva, S.V. Larionov, Koord. Khimiya 16 (1990) 654.
[30] L.G. Lavrenova, N.G. Yudina, V.N. Ikorskii, V.A. Varnek, I.M. Oglezneva, S.V. Larionov, Polyhedron 14 (1995) 1333.
[31] O. Roubeau, J.M.A. Gomez, E. Balskus, J.J.A. Kolnaar, J.G. Haasnoot, J. Reedijk, New J. Chem. 25 (2001) 144.
[32] W. Vreugdenhil, J.G. Haasnoot, O. Kahn, P. Thuéry, J. Reedijk, J. Am. Chem. Soc. 109 (1987) 5272.
[33] W. Vreugdenhil, J.H. van Diemen, R.A.G. de Graaff, J.G. Haasnoot, J. Reedijk, A.M. van der Kraan, O. Kahn, J. Zarembowitch, Polyhedron 9 (1990) 2971.
[34] A. Ozarowski, S.Z. Yu, B.R. McGarvey, A. Mislankar, J.E. Drake, Inorg. Chem. 30 (1991) 3167.
[35] Y. Garcia, O. Kahn, L. Rabardel, B. Chansou, L. Salmon, J.P. Tuchagues, Inorg. Chem. 38 (1999) 4663.
[36] V. Niel, Transiciones de Espin en Complejos de HIerro (II) Inducidas por la accion de la Temperatura, la presion y la luz, Ph.D Thesis, Universidad Valencia, Valencia, 2002.
[37] V. Niel, A. Galet, A.B. Gaspar, M.C. Muñoz, J.A. Real, Chem. Commun. (2003) 1248.
[38] V. Niel, J.M. Martinez-Agudo, M.C. Muñoz, A.B. Gaspar, J.A. Real, Inorg. Chem. 40 (2001) 3838.
[39] V. Niel, M.C. Muñoz, A.B. Gaspar, A. Galet, G. Levchenko, J.A. Real, Chem.-Eur. J. 8 (2002) 2446.
[40] P.J. van Koningsbruggen, Y. Garcia, O. Kahn, L. Fournès, H. Kooijman, A.L. Spek, J.G. Haasnoot, J. Moscovici, K. Provost, A. Michalowicz, F. Renz, P. Gütlich, Inorg. Chem. 39 (2000) 1891.
[41] P.J. van Koningsbruggen, Top. Curr. Chem. 233 (2004) 259.
[42] P.J. van Koningsbruggen, Y. Garcia, H. Kooijman, A.L. Spek, J.G. Haasnoot, O. Kahn, J. Linarès, E. Codjovi, F. Varret, J. Chem. Soc., Dalton Trans. (2001) 466.
[43] J. Schweifer, P. Weinberger, K. Mereiter, M. Boca, C. Reichl, G. Wiesinger, G. Hilscher, P.J. van Koningsbruggen, H. Kooijman, M. Grunert, W. Linert, Inorg. Chim. Acta 339 (2002) 297.
[44] C.M. Grunert, J. Schweifer, P. Weinberger, W. Linert, K. Mereiter, G. Hilscher, M. Müller, G. Wiesinger, P.J. van Koningsbruggen, Inorg. Chem. 43 (2004) 155.
[45] I. Lawthers, J.J. Mcgarvey, J. Am. Chem. Soc. 106 (1984) 4280.
[46] J.J. Mcgarvey, I. Lawthers, K. Heremans, H. Toftlund, Chem. Commun. (1984) 1575.
[47] S. Decurtins, P. Gütlich, C.P. Köhler, H. Spiering, A. Hauser, Chem. Phys. Lett. 105 (1984) 1.
[48] A. Hauser, J. Chem. Phys. 94 (1991) 2741.
[49] I.M. Kolthoff, P.J. Elving (Eds.), Treatise on Analytical Chemistry, vol. 4, Wiley, New York, 1963.
[50] R.J. Cernik, W. Clegg, C.R.A. Catlow, G. Bushnell Wye, J.V. Flaherty, G.N. Greaves, I. Burrows, D.J. Taylor, S.J. Teat, M. Hamichi, J. Synchrot. Radiat. 4 (1997) 279.
[51] SAINT, Siemens Analytical X-ray Instruments Inc., Madison, Wisconsin.
[52] G. Aromi, J. Ribas, P. Gamez, O. Roubeau, H. Kooijman, A.L. Spek, S. Teat, E. MacLean, H. Stoeckli-Evans, J. Reedijk, Chem.-Eur. J. 10 (2004) 6476.
[53] R. Bronisz, Eur. J. Inorg. Chem. (2004) 3688.
[54] P. Gütlich, A. Hauser, Coord. Chem. Rev. 97 (1990) 1.
[55] P. Gütlich, Struct. Bond. 44 (1981) 83.
[56] A.F. Stassen, O. Roubeau, I.F. Gramage, J. Linarès, F. Varret, I. Mutikainen, U. Turpeinen, J.G. Haasnoot, J. Reedijk, Polyhedron 20 (2001) 1699.
[57] O. Roubeau, A.F. Stassen, I.F. Gramage, E. Codjovi, J. Linarès, F. Varret, J.G. Haasnoot, J. Reedijk, Polyhedron 20 (2001) 1709.
[58] J.F. Létard, L. Capes, G. Chastanet, N. Moliner, S. Letard, J.A. Real, O. Kahn, Chem. Phys. Lett. 313 (1999) 115.
[59] A. Absmeier, M. Bartel, C. Carbonera, G.N.L. Jameson, P. Weinberger, A. Caneschi, K. Mereiter, J.-F. Létard, W. Linert, Chem. - Eur. J. 12 (2006) 2235.
[60] J.F. Létard, P. Guionneau, L. Rabardel, J.A.K. Howard, A.E. Goeta, D. Chasseau, O. Kahn, Inorg. Chem. 37 (1998) 4432.
[61] S.V. Voitekhovich, P.N. Gaponik, D.S. Pytleva, A.S. Lyakhov, O.A. Ivashkevich, Pol. J. Chem. 76 (2002) 1371.

[62] R. Bronisz, Inorg. Chim. Acta 340 (2002) 215.

[63] R. Bronisz, Inorg. Chim. Acta 357 (2004) 396.

[64] G.A. van Albada, O. Roubeau, I. Mutikainen, U. Turpeinen, J. Reedijk, New J. Chem. 27 (2003) 1693.

[65] F.S. Keij, R.A.G. de Graaff, J.G. Haasnoot, A.J. Oosterling, E. Pedersen, J. Reedijk, J. Chem. Soc., Chem. Commun. (1988) 423.

[66] W.B. Sharp, P. Legzdins, B.O. Patrick, J. Am. Chem. Soc. 123 (2001) 8143.

[67] H. Casellas, A. Pevec, B. Kozlevcar, P. Gamez, J. Reedijk, Polyhedron 24 (2005) 1549.

[68] H.M. Seo, S.G. Lee, D.M. Shin, B.K. Hong, S.G. Hwang, D.S. Chung, Y.K. Chung, Organometallics 21 (2002) 3417.

[69] L. Carlucci, G. Ciani, D.M. Proserpio, S. Rizzato, CrystEngComm (2002) 121.

[70] P.J. van Koningsbruggen, M. Grunert, P. Weinberger, Mon. Chem. 134 (2003) 183.

[71] Y. Garcia, V. Niel, M.C. Muñoz, J.A. Real, Top. Curr. Chem. 233 (2004) 229.

[72] Y. Garcia, V. Ksenofontov, G. Levchenko, P. Gütlich, J. Mater. Chem. 10 (2000) 2274.

[73] J.F. Létard, P. Guionneau, O. Nguyen, J.S. Costa, S. Marcen, G. Chastanet, M. Marchivie, L. Goux-Capes, Chem. -Eur. J. 11 (2005) 4582.

[74] A. Hauser, A. Vef, P. Adler, J. Chem. Phys. 95 (1991) 8710.